Using a New Mixture of Reagents for Effective Inhibition of Corrosion and Salt Precipitation in the Petroleum Industry

Azizollah Khormali *

1. Department of chemistry, Faculty of basic sciences and engineering, Gonbad Kavous University, Gonbad Kavous, Iran. E-mail: a.khormali@gonbad.ac.ir

ARTICLE INFO	ABSTRACT
	In recent years, universal inhibitors capable of inhibiting corrosion and salts have attracted much attention in the petroleum industry. In this work, various industrial scale and corrosion inhibitors were used to develop a new mixture of reagents to prevent calcium carbonate, barium sulfate, calcium sulfate, and corrosion. The developed mixture of reagents (named DAHAPZ) consists of the following components: DTPMP, ATMP, HEDP, 2-aminoN-decyl-3-phenyl propionamide, 2-propyl-3-ethyl-8-oxychinolin – $ZnCl_2$. When using DAHAPZ, an inhibition efficiency of more than 92% was observed for salts of $CaCO_3$, $BaSO_4$, and $CaSO_4$) and corrosion (for a steel carbon in an acidic environment). After the application of DAHAPZ, the corrosion rate was reduced from 2 mm/year to 0.04 mm/year (an efficiency of 98%). The results of the impedance spectrum test showed that the optimal concentration of DAHAPZ for effective inhibition is 30 ppm. Furthermore, the turbidity test and the measurement of the number of precipitated salts confirmed the high inhibition performance of DAHAPZ to prevent salt precipitation. DAHAPZ inhibits the salt crystals which could serve as a protective barrier, thereby reducing the corrosion rate at various temperatures. The deceleration of the crystal growth rate when using DAHAPZ is associated with effective adsorption on the crystals, and a decrease in the crystal surface area for growth. Also, the results of coreflood experiments on the adsorption of the reagents onto the carbonate and sandstone rocks showed that DAHAPZ is more suitable to be used in carbonate reservoirs.

Introduction

The continuous growth of salt precipitation and corrosive destruction of underground equipment has become a serious problem in the petroleum industry. Corrosion and salt precipitation can occur during oil production at all stages of the field development [1–6]. Annually, many electrical submersible pumps (ESP) failures occur due to corrosion, and the precipitations of various types of inorganic salts. The salt precipitation in the near-wellbore region and the production equipment decreases the production rate. Amro [7] reported a 90% reduction in rock permeability due to salt precipitation, indicating that it needs to be controlled before formation. The lifetime of the production equipment can be reduced significantly due to the salt precipitation and corrosion problem. Therefore, it is impossible to extend the life of the equipment without protection against scale and corrosion [8–12].

---

* Corresponding Author: A. Khormali (E-mail address: a.khormali@gonbad.ac.ir)

The salt precipitates are characterized by rather complex structures, including insoluble impurities, organic, and inorganic components. The inorganic salts in the petroleum industry are classified according to their chemical composition as follows: sulfate, carbonate, chloride, and sulfide types [1, 13, 14]. Calcite, aragonite, and vaterite are three different forms of calcium carbonate salts. The precipitation of salt is strongly dependent on the crystallization conditions and the ionic composition of the brines [2, 15, 16]. Furthermore, sulfate salts are commonly found in calcium sulfate, barium sulfate, and strontium sulfate in the oil industry. Supersaturation is the primary cause of inorganic salt formation. When the saturation level of the brine is higher than the supersaturation level, many small particles, which act as a crystallization center, appear instantly [17, 18]. Depending on the type of inorganic salt, various parameters can affect the process of salt precipitation due to supersaturation and a decrease in solubility. Some of them are: temperature, pressure, ion content, the mixing ratio of formation and injection waters, presence of carbon dioxide, changes in pH of the brines, contact time, hydrodynamic factors [7, 19–21].

Corrosion is a process, during which the materials are destroyed by interacting with an aggressive medium. The corrosion of the equipment is affected by many parameters, including pressure, temperature, change in the water cut, presence of salts and mechanical impurities, formation water components, flow parameters, presence of natural gases, cationic and anionic species, type of surface material, pH, and the presence of pre-corrosion products [9, 22, 23]. The main corrosion mechanisms due to the gas dissolved in the water are associated with the following materials: carbon dioxide, hydrogen sulfide, and oxygen [24, 25]. The corrosion damage to production equipment is determined by the physicochemical properties of the water and hydrocarbon components [26, 27]. In a mineralized aqueous medium, the interaction of an electrolyte with metal leads to corrosion, which takes place by an electrochemical mechanism. In this case, corrosion reactions can be divided into two simultaneously occurring processes — anodic and cathodic. Production equipment made of dissimilar metals is a multi-electrode element in which anodes and cathodes alternate [23, 28].

The chemical method is the most rational and effective way to control the scale and corrosion in the petroleum industry. The use of chemical inhibitors is the most efficient method for preventing corrosion and salt precipitation in the well and reservoir [2, 29–31]. Currently, there is a fairly large set of inhibitors that have different inhibition mechanisms. The injection of an effective inhibitor into the well completely prevents corrosion and salt precipitation in the production system. To effectively protect the equipment against salt and corrosion, a suitable inhibitor must always be present in the system at a minimum inhibitory concentration [6, 23, 32, 33]. Ahmed et al. [20] reported a significant improvement in the surface morphology characteristics of the reservoir rock and a decrease in the accumulated salts (pyrite) after the use of inhibitors.

To achieve the maximum protective effect of a scale inhibitor, it should be injected into the well before the crystallization of the inorganic salts. The inhibition efficiency of a scale inhibitor is dependent on its nature, inhibition mechanism, the capacity for the adsorption onto the rock surface, and the type of salt [1, 13, 34, 35]. The essence of the inhibition of salt precipitation with the use of reagents is associated with a change in the solubility of salt in the brine [36, 37]. Phosphonic and carboxylic acids are the most widely used scale inhibitors in the petroleum industry. The main advantage of these scale inhibitors is their high efficiency at relatively low concentrations. Various parameters can affect the scale inhibition efficiency. Some of them are: retention time, pH, temperature, type and concentration of additives, chemical structure, level of brine supersaturation with ions [2, 15, 16, 34].

The use of the corrosion inhibitors provides the effective and reliable protection of the equipment against damage and increases the mean time between failures (MTBF). The

corrosion inhibitors should reduce the corrosion rate as much as possible without adversely affecting the equipment. The inhibition mechanism of the corrosion inhibitors can be explained by the adsorption processes, owing to which a protective layer is formed on the surface of the equipment [27, 38–40]. Also, their inhibition mechanism may be associated with a decrease in the interfacial tension at the oil-water interface or an increase in the wetting ability of oil in relation to the metals. The inhibition mechanism of the corrosion inhibitors is dependent on the composition, structure, and properties of the molecules [41, 42]. The corrosion inhibitors, which are widely used in the oil industry, may include organic compounds exhibiting an inhibitory effect, water-alcohol or hydrocarbon solvents, and various additives in order to control their properties during the inhibition process [32, 38, 43, 44]. Moreover, high molecular weight amines, imidosalines, phosphorus-containing compounds, and other organic materials are used as active components of the corrosion inhibitors [11, 45, 46].

The complications associated with corrosion and salt precipitation in the production equipment are closely related. Scale inhibitors may damage the equipment by increasing the corrosion rate if they contain acidic components [36, 47, 48]. The solution to this problem is using a mixture of reagents that inhibit corrosion and salt precipitation. The application of such mixtures can provide reliable protection of the downhole equipment, increase MTBF and reduce the costs associated with selecting and injecting many inhibitors for various purposes [3, 18, 21, 31, 45, 49–51]. Al-Sabagh et al. [26] reported a high inhibition efficiency for preventing both corrosion and salt precipitation by using a hexa-anionic surfactant for an extended period without any negative impact on the production performance. Dong et al. [43] investigated the inhibition of calcium carbonate precipitation and the corrosion in a carbon steel sample using a mixture of reagents, including various functional groups. They observed an inhibition efficiency of over 94% for both scale and corrosion at 80 °C and 50 mg/L of the inhibitor. Sabzi and Arefnia [45] could enhance the inhibition efficiency to control corrosion and calcium carbonate precipitation using zinc ions, the mechanism of which was based on reducing both nucleation and crystal growth rates (for scale), as well as blocking cathodic sites (for corrosion). Gutierrez et al. [31] examined various reagents for both scale and corrosion inhibition. They could prevent corrosion and salt precipitation, obtaining a synergistic effect among the reagents at a specific concentration. In the literature, a mixture of reagents for the inhibition of calcium and sulfate salts, and also, corrosion was not reported.

In this work, an effective mixture of reagents was developed to inhibit three types of salts (calcium carbonate, barium sulfate, calcium sulfate) and corrosion in the oil industry. For this purpose, various industrial scale and corrosion inhibitors were used, and their inhibition performance was evaluated. The corrosion rate in the presence of the developed mixture of reagents was determined at various concentrations in order to obtain its optimal concentration. Moreover, the impedance spectrum in the presence of DAHAPZ was investigated to prevent corrosion. The next objective of this work was to study the effect of temperature on the inhibition performance of DAHAPZ under static conditions. The turbidity in the brines was examined with and without the use of DAHAPZ. The final objective was to determine the adsorption and desorption kinetics of DAHAPZ on the carbonate and sandstone rocks through coreflood tests.

Materials and methods

Materials (Brines, Scale and Corrosion Inhibitors)

Three different brines were prepared to develop an effective mixture of reagents for salt and corrosion inhibition and to evaluate its performance. Each brine had a high tendency to form and precipitate a certain salt. The ionic composition of the synthetic brines prone to the precipitation of calcium carbonate, barium sulfate and calcium sulfate salts is shown in Table

1. The first brine was prone to calcium carbonate precipitation, the second brine to barium sulfate, and the third brine to calcium sulfate.

Table 1. The ionic composition of the used brines

Brine No.	pH	Cl⁻	HCO₃⁻	SO₄²⁻	K⁺	Na⁺	Mg²⁺	Ca²⁺	Ba²⁺
				Ion concentration, mg/L					
1 (for CaCO₃)	6.95	32565	859	0	98	7254	112	325	0
2 (for BaSO₄)	6.70	33654	325	1050	117	6258	152	0	269
3 (for CaSO₄)	6.46	30256	0	1542	112	7450	109	657	0

Various scale and corrosion inhibitors were used to develop an effective mixture of reagents for inhibiting both corrosion and salt precipitation. These reagents are presented in Table 2.

Table 2. Scale and corrosion inhibitors

Reagent abbreviation		Name
Scale inhibitor	DTPMP	diethylenetriamine penta
	HDTMP	hexamethylenediaminotetra (methylene phosphonic acid)
	PBTC	2-phosphonobutane-1,2,4-tricarboxylic acid
	HEDP	hydroxyethylidenediphosphonic acid
Corrosion inhibitor	-	2-aminoN-decyl-3-phenyl propionamide
	-	benzalkonium chloride
	-	2-propyl-3-ethyl-8-oxychinolin – ZnCl₂

Determination of the scale of inhibition performance

The jar tests were carried out to determine the inhibition efficiency of the salt precipitation under static conditions. The test methodology is based on assessing the ability of inhibitors to keep the cations in suspension. In the tests, the concentration of cations of Ca^{2+} (for calcium carbonate and calcium sulfate), and Ba^{2+} (for barium sulfate) in the working solution was measured in the following three cases: i) before the test conduction (K_i); ii) after the test conduction with the use of the inhibitor (K_{f2}); iii) after the test conduction without the use of the inhibitor (K_{f1}). Working solutions with and without scale inhibitors were kept in an oven at the desired temperature for 24 hours. This time is sufficient to prevent salt precipitation using scale inhibitors under static conditions [4]. After 24 hours, the working solutions were filtered through a filter paper. Thereafter, they were immediately analyzed for residual calcium and barium ions. The concentration of the cations in the working solutions was determined by using a pH/ion meter. The inhibition performance for the scale prevention was calculated as follows:

$$SIE = \frac{K_{f2} - K_{f1}}{K_i - K_{f1}} 100\%$$

(1)

where *SIE* is the scale inhibition performance; K_{f2} and K_{f1} are the concentrations of the cations after the test conduction in the presence and absence of the reagents, respectively; K_i is the initial concentration of the reagents before the test conduction.

The jar tests were completed using the reagents at concentrations of 10, 20, 30, 40, and 50 ppm. The tests were conducted at 60 °C, and atmospheric pressure (based on the standard of NACE TM0374-2016). It should be noted that the solubility of calcium sulfate and barium sulfate is approximately independent of pressure. But the solubility of calcium carbonate is increased by increasing pressure [52–54]. Thus, at low pressures, the maximum amount of calcium carbonate is precipitated.

In addition, to analyze the influence of the temperature on the inhibition performance of the developed mixture, the jar tests were repeated in a temperature range from 40 °C to 120 °C

(Table 4). Also, the salt concentration (calcium carbonate, calcium sulfate, barium sulfate) was examined in the presence and absence of scale inhibitor by measuring the mass of the precipitated salts. In this case, the scale inhibitor was used at a constant concentration of 30 ppm (Fig. 11). The temperature and experiment duration was 60 °C, and 24 hours, respectively. It should be noted that the possibility of salt precipitation was examined using the OLI Studio program. The results showed that at the investigated temperature range and pressure in the used brines, a sufficient amount of calcium carbonate, calcium sulfate, and barium sulfate precipitation was predicted.

Analysis of the Corrosion Rate and the Corrosion Inhibition Efficiency

The gravimetric method is the simplest method for determining the corrosion rate. However, it provides reliable information only if the corrosion is uniform and spreads over the entire surface. The method is based on immersing metal samples of known geometric dimensions in a potentially aggressive environment for a specific time. The reduction in the mass of the samples during this time is used to calculate the average corrosion rate. The gravimetric method was used to evaluate the corrosion rate of carbon steel samples (grade L80) and the corrosion inhibition performance under laboratory conditions. The samples were prepared with a size of 2.0 cm × 2.0 cm × 0.3 cm. The method includes determining the mass loss of the carbon steel samples after the immersion in an acidic solution (1 M HCl) with and without the use of the inhibitors. Immediately after each test, the samples were visually inspected for the presence of the corrosion products. The corrosion rate of the samples was calculated using the fowling formula:

$$R_{corr} = 8760 \frac{m_i - m_f}{A.t.\rho} \tag{2}$$

where R_{corr} is the corrosion rate, mm/year; m_f and m_i are the masses of the carbon steel samples after and before the test, gr; A is the surface area of the samples, m^2; t is the test duration, hour; ρ is the density of the samples, 7870 kg/m^3.

The corrosion rate test was repeated three times at each concentration of the inhibitors. Thus, the corrosion rate was determined by calculating the arithmetic mean of the experimental data obtained in each test. The permissible difference between, which did not exceed 3% (with a 95% confidence level). The experiment duration of the corrosion rate analysis was 48 hours. The corrosion rate measurement was completed by using a laboratory balance with an accuracy of 0.001 gr. The tests were completed at a reservoir temperature of 60 °C, and atmospheric pressure. Initially, the corrosion rate tests were carried out in the absence of the developed mixture. Then, the tests were continued using the mixture of regents at concentrations of 10, 20, 30, 40, and 50 ppm. Moreover, it should be noted that the self-corrosion rate of the used carbon steel samples was evaluated by the linear polarization method. The rate of this type of corrosion was relatively low and constant during the tests and did not significantly affect the salt precipitation and inhibition.

The corrosion inhibition performance was calculated using the following formula:

$$CIE = \frac{R_{corr1} - R_{corr2}}{R_{corr1}} \times 100\% \tag{3}$$

where CIE is the corrosion inhibition performance, R_{corr1} and R_{corr2} are the corrosion rates in the absence and presence of the inhibitor, mm/year.

To determine the corrosion inhibition performance, the corrosion rates were examined with and without using the inhibitors at 60 °C. The duration of each test was 48 hours. The inhibitors were added to the working solutions at concentrations of 10, 20, 30, 40, and 50 ppm. In addition, to study the effect of temperature on the inhibition performance of the developed mixture, the

corrosion inhibition efficiency was evaluated in a temperature range from 40 °C to 120 °C at 30 ppm (Table 4).

Measurement of Electrochemical Impedance Spectroscopy (EIS), and Turbidity

EIS tests were carried out in a conventional three-electrode cell (counter, reference and working electrodes) and potentiostat, in which the carbon steel samples were used as the working electrode. A schematic of the experimental setup used for the EIS test is shown in Fig. 1. The dynamics of the potential changes in the corrosive environment were studied in the presence of the inhibitor. For this purpose, the developed mixture was added to the solution at concentrations of 10, 20, 30, and 40 ppm. The working solution (electrolyte) was 1 M HCl. The studies by the potentiodynamic method were carried out in the following order: the carbon steel samples (as working electrodes) were polished with sandpaper and fixed in an electrochemical cell. A potentiostat device was connected to a special computer program and the electrodes with the corresponding cables. The samples were immersed in the solution for four hours. Then, an open circuit potential was recorded for one hour to obtain a steady-state condition. Finally, EIS tests were completed using the open circuit potential in a frequency range from 10^{-5} Hz to 10^{-1} Hz at five mV. The potential of the solution was indicated by the computer program at all studied concentrations. The tests were repeated three times to maximize the accuracy of the results. The arithmetic mean of the experimental data obtained at each concentration was calculated.
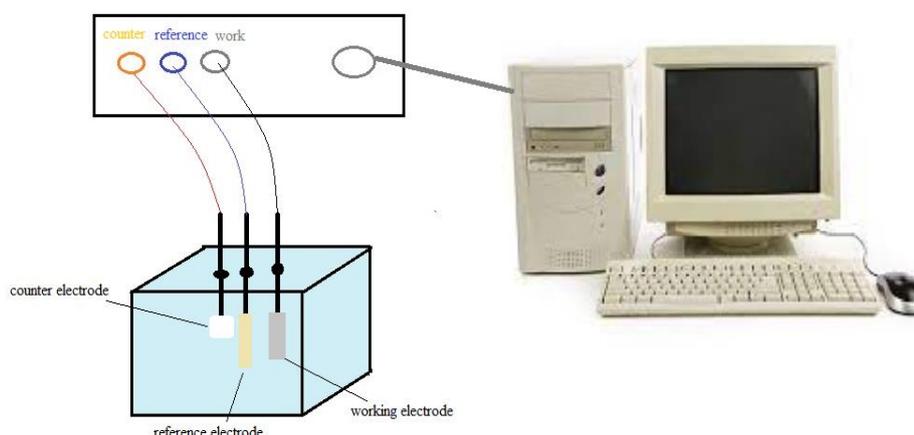
Fig. 1. Schematic of the experimental setup used for EIS tests

Turbidity is one of the most important parameters for evaluating the scale inhibition performance under static conditions. Turbidity analysis includes the determination of the amount of light scattered through a working solution containing the suspended particles. This test is the result of the interaction between the light and particles suspended in a brine. If the sample contains suspended solids, the result of the interaction of the sample with transmitted light depends on the size, shape and composition of the particles. A high-accuracy turbidity meter of HI88713 was used to measure the turbidity values in the brines with and without the use of the inhibitor (Fig. 2). In this apparatus, the turbidity values were determined photometrically. The apparatus contains a radiation source and a detector that measures the intensity of this radiation. Thus, the scattered light was assessed by the detector, which is located at an angle of 90 from the light source. The detector had sensitivity in a range from 400 nm to 700 nm. The basic principle of operation of the turbidity meter is the measurement of the optical density with a subsequent digital presentation of the results. The turbidity tests were

completed with and without the use of the developed mixture at 60 °C and atmospheric pressure. In this experiment, all brines (No. 1–3) were examined to analyze the inhibition of calcium carbonate, calcium sulfate, and barium sulfate salts. Turbidity tests were performed immediately after preparing the brines in order to prevent the influences of temperature and particle settling on the turbidity value. Temperature changes can affect the solubility of salts in the brines. The developed mixture of reagents (DTPMP, ATMP, HEDP, 2-aminoN-decyl-3-phenyl propionamide, 2-propyl-3-ethyl-8-oxychinolin – $ZnCl_2$) was added to the brines at a constant concentration of 30 ppm. The duration of each test was 200 min. This time is sufficient to evaluate the performance of scale inhibitors in turbidity tests [55].

Fig. 2. The used turbidity meter

Coreflood Experiment Conduction

The adsorption and desorption properties of the developed mixture under dynamic conditions were evaluated on the rock surfaces using a coreflood apparatus. A schematic of the experimental setup used for coreflood tests is shown in Fig. 3. A high-pressure pump, coreholder, tank, a sensor for temperature measurement, and pressure transducer were the main components of the used coreflood apparatus. The coreflood apparatus allows simulating the fluid flow through a core sample at a temperature and pressure as close as possible to the reservoir conditions. The apparatus had an automated pressure control system that regulates and measures the pressure with time. The working agent of the pump is oil, under the action of which the piston was squeezed out, displacing the solutions from the tank into the core samples. In this work, to determine the adsorption and desorption profiles of the inhibitor, the following rock samples were used: carbonate (porosity–16%, permeability–26 mD), and sandstone (porosity–13%, permeability–19 mD). The average diameter, length and mass of the rock samples were 3 cm, 6 cm, 95 gr, respectively. The preparation of core samples, as well as the coreflood tests were carried out in accordance with the standards. The tests were completed at 60 °C, and an injection rate of 3 mL/min. To evaluate the adsorption process onto the rock surface, brine No.1 containing the developed mixture at 30 ppm was injected into the core samples for 60 min. During the adsorption process, the inhibitor concentration per mass of the core samples was determined for 1 hour. Then, to assess the desorption process, brine No.1 was injected into the core samples without adding the developed mixture for 120 min. The profile of the adsorption and desorption processes during the coreflood experiments was determined by measuring the inhibitor content at the outlet of the coreholder. The concentration of DAHAPZ in the coreflood tests was determined by measuring only the concentration of phosphonate reagents. At the outlet of the coreholder, the concentration of the phosphate ions was evaluated by titration.
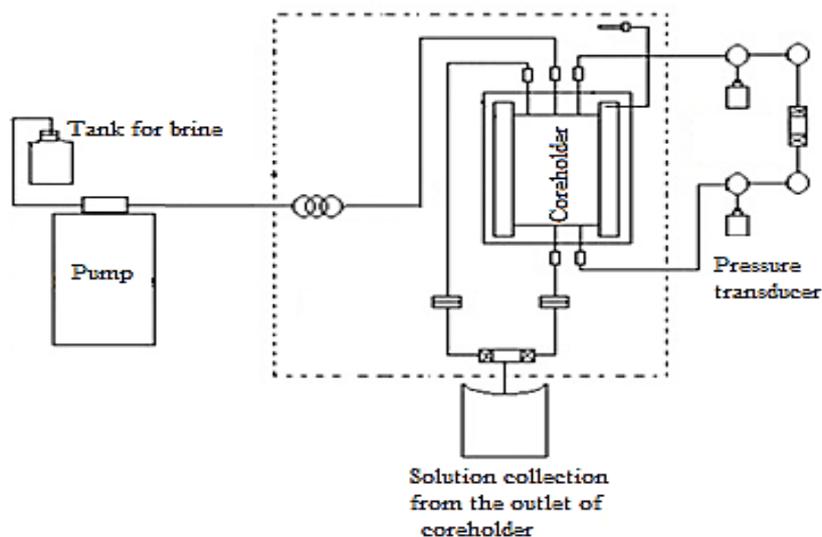
Fig. 3. Schematic of the experimental setup used for coreflood test

Results and Discussion

Development of the Mixture of Reagents for the Inhibition of Salt and Corrosion

A set of static tests was carried out in order to obtain the optimal formulation for the effective prevention of corrosion and salt precipitation (calcium carbonate, barium sulfate, calcium sulfate). In accordance with the standards for the use of scale and corrosion inhibitors, the inhibition efficiency of the reagents should be at least 90% under laboratory conditions. Three mixtures of scale inhibitors (SI) and four mixtures of corrosion inhibitors (CI) were prepared to develop an effective inhibitor package and evaluate its performance. These mixtures are shown in Table 3. The mixing ratios of SIs and CIs were 1:1:1 and 1:1.

Table 3. Mixtures of scale and corrosion inhibitors

Scale (SI) and Corrosion (CI) Inhibitors	
SI No.1	DTPMP + ATMP + PBTC
SI No.2	DTPMP + ATMP + HEDP
SI No.3	PBTC + ATMP + HEDP
CI No.1	2-aminoN-decyl-3-phenyl propionamide + ethanol
CI No.2	2-aminoN-decyl-3-phenyl propionamide + 2-propyl-3-ethyl-8-oxychinolin – $ZnCl_2$
CI No.3	benzalkonium chloride + 2-propyl-3-ethyl-8-oxychinolin – $ZnCl_2$
CI No.4	2-aminoN-decyl-3-phenyl propionamide + benzalkonium chloride

Figs. 4 to 6 present the inhibition performance of the prepared mixtures of SI and CI for preventing salt and corrosion at various concentrations at 60 °C. SI and CI were mixed in a ratio of 1:1. All tests were conducted in accordance with the standard methods and procedures for salt and corrosion prevention under static conditions. The inhibition performance was determined using Equations 1 and 3. In this work, it was aimed to develop a mixture of reagents for effective inhibition of $CaCO_3$, $BaSO_4$, and $CaSO_4$ salts, and corrosion. Fig. 4 shows the results of the inhibition performance of SI No.1 (DTPMP + ATMP + PBTC) in the presence of all corrosion inhibitors (CIs No.1–4). As presented in the figure, in all cases, the mixtures could not demonstrate high inhibition performance for preventing salt precipitation. The scale inhibition efficiency was lower than 90%. The lowest scale inhibition efficiency in preventing calcium carbonate salt precipitation was observed for the mixture of SI No.1 (DTPMP + ATMP + PBTC) and the corrosion inhibitors.

Moreover, high corrosion inhibition performance was obtained using the mixture of SI No.1 and CI.2. In this case, the corrosion inhibition efficiency was 90% at 40 mg/L. Therefore, the mixtures of SI No.1 and the corrosion inhibitors were not highly effective in preventing both corrosion and salt precipitation.
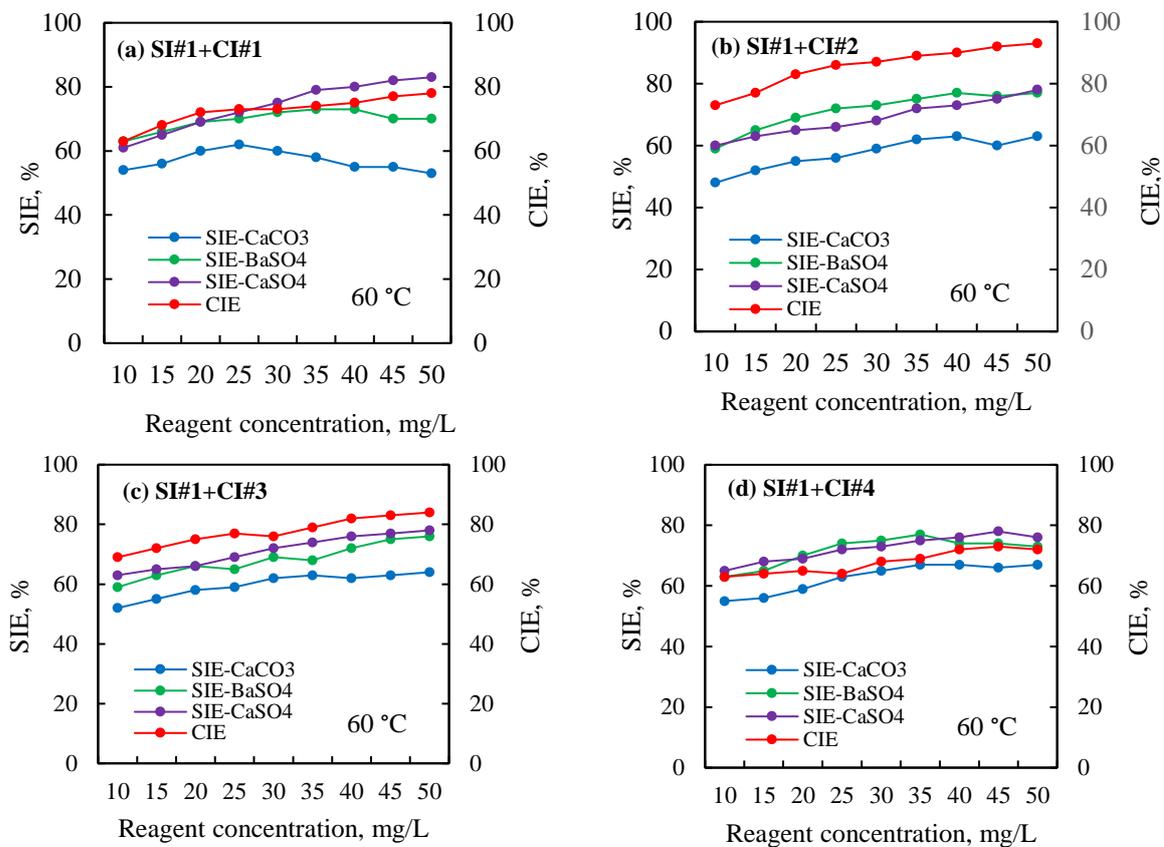
Fig. 4. The changes in the inhibition performance of salt precipitation and corrosion with the use of SI No.1 and Cis

At the next stage, mixtures of SI No.2 (DTPMP + ATMP + HEDP) and all corrosion inhibitors (CIs No.1–4) were examined at various concentrations. The results obtained for the prevention of corrosion and salt precipitation are shown in Fig. 5. These mixtures were more effective than SI No.1 in inhibiting salt precipitation. Among the studied mixtures, a mixture of SI No.2 and CI. No.2 had the highest inhibition efficiency in preventing both scale and corrosion. In this case, at concentrations above 30 mg/L, the inhibition performance in preventing calcium carbonate, barium sulfate, calcium sulfate, and corrosion was more than 90%. The high efficiency in preventing salt precipitation was achieved, since the crystallization process was inhibited by the effective mechanism of the investigated reagents, providing a positive synergistic effect. In addition, the adsorption of the reagents could play an important role in inhibiting $CaCO_3$ and $BaSO_4$ and $CaSO_4$ salt precipitation. Therefore, the mixture of SI No.2 and CI No.2 can effectively inhibit corrosion and salt precipitation.
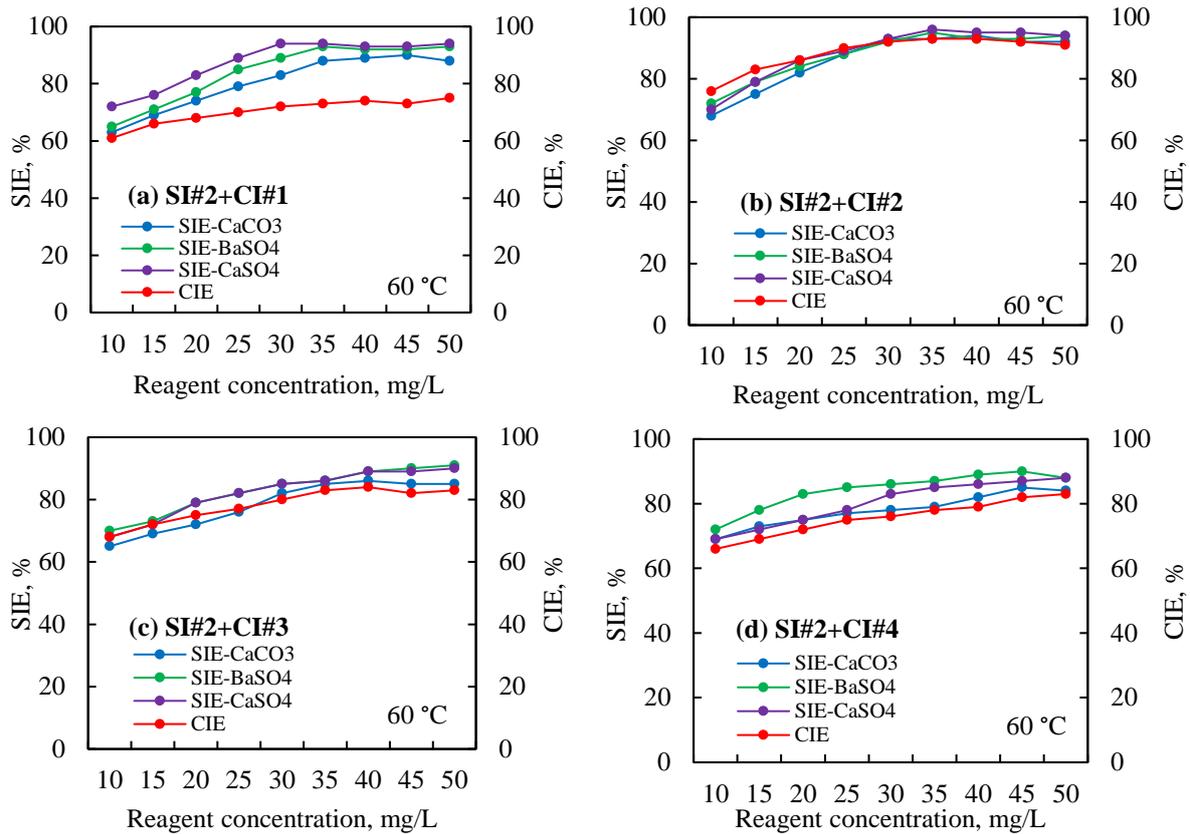
Fig. 5. The changes in the inhibition performance of salt precipitation and corrosion with the use of SI No.2 and CIs

To analyze the inhibition performance of mixtures of SI No.3 (PBTC + ATMP + HEDP) and all corrosion inhibitors (CIs No.1–4), the static tests were carried out at a constant temperature of 60 °C and concentrations of 10, 20, 30, 40, and 50 ppm. The results are shown in Fig. 6. As presented in the figure, the inhibition efficiency was not high enough to prevent barium sulfate precipitation.
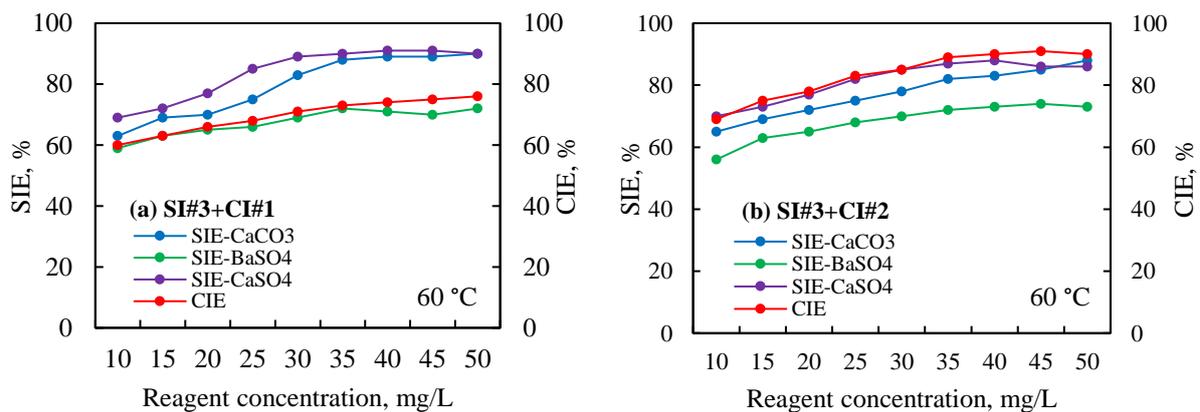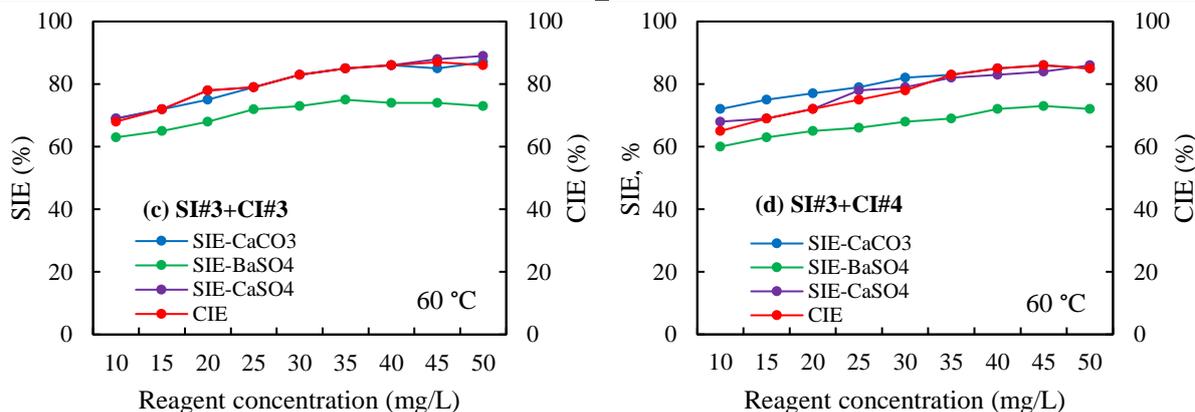
Fig. 6. The changes in the inhibition performance of salt precipitation and corrosion with the use of SI No.3 and CIs

Fig. 7 depicts the inhibition performance of the developed mixture of reagents (DAHAPZ) at various mixing ratios of SI No.2 (DTPMP + ATMP + HEDP), and CI No.2 (2-aminoN-decyl-3-phenyl propionamide + 2-propyl-3-ethyl-8-oxychinolin – ZnCl2). The tests were carried out at a concentration and temperature of 30 ppm and 60 °C under static conditions. In the tests, the mixing ratio of DTPMP, ATMP, and HEDP were 1:1:1. Also, the mixing ratio of 2-aminoN-decyl-3-phenyl propionamide and 2-propyl-3-ethyl-8-oxychinolin – ZnCl2 was 1:1. It should be noted the mixing ratios of SI and CI were selected at equal intervals (10:90; 15:85; 20:80; …; 90:10). But they are not presented in the figure due to large data and columns. As shown in the figure, in a ratio of 25:75 of SI:CI, there was a low level of inhibition efficiency in preventing salt precipitation. Moreover, in a ratio of 75:25 of SI:CI, the corrosion inhibition performance was low. Among the investigated ratios, the highest inhibition performance in preventing both corrosion and salt precipitation was observed in a ratio of 50:50 of SI:CI. Thus, the scale and corrosion inhibitors were mixed in a ratio of 50:50. Accordingly, the mass concentration of the components of DAHAPZ is: DTPMP–16.6%, ATMP–16.7%, HEDP–16.7%, 2-aminoN-decyl-3-phenyl propionamide–25%, 2-propyl-3-ethyl-8-oxychinolin – ZnCl2–25%.

Therefore, the mixture of SI No.2 + CI No.2, which had the highest inhibition efficiency in preventing both corrosion and salt precipitation, is used in the next experiments. The technical result of DAHAPZ is to achieve a dual inhibitory effect: inhibition of salt precipitation (calcium carbonate, barium sulfate, calcium sulfate) and corrosion. Thus, the inhibition performance of DAHAPZ is evaluated by conducting various tests at different concentrations.
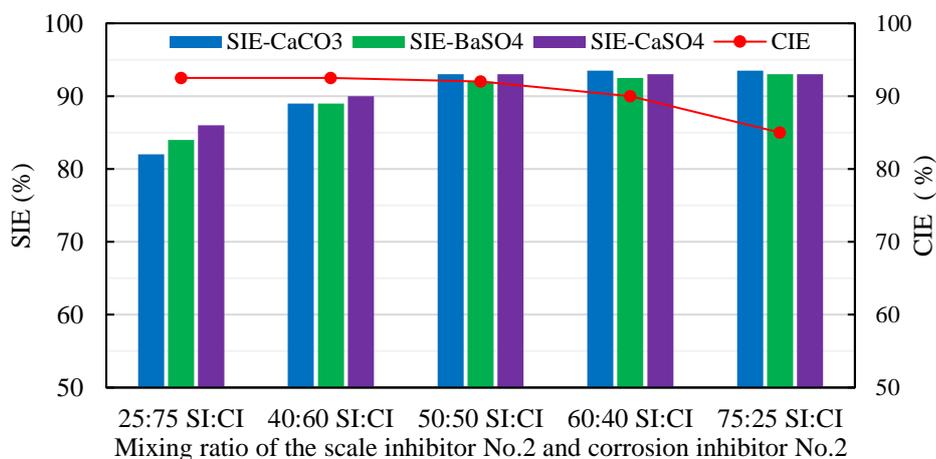
Fig. 7. The dependence of the inhibition performance on the mixing ratio of SI and CI at a concentration and temperature of 30 ppm and 60 °C

The Results of the Determination of the Corrosion Rate and EIS Tests

The corrosion rate of the carbon steel samples was evaluated at various concentrations of DAHAPZ. For this purpose, the corrosion rate was determined before and after adding DAHAPZ to the working solution. The maximum protective properties of an inhibitor are achieved when it is introduced into an aggressive environment in an amount sufficient to cover the surface of the samples with a monomolecular layer [56]. Figure 8a shows the changes in the corrosion rate of the samples in the presence and absence of DAHAPZ. As presented in the figure, the corrosion rate was increased over time in the absence of DAHAPZ. This can be explained by the fact that the interaction of the carbon steel samples with an acidic environment may be increased with time. The corrosion rate in the absence of DAHAPZ has reached more than 2 mm/year after 8 hours. This value is the high corrosion rate in the petroleum industry. Then, to reduce the corrosion rate, DAHAPZ was added to the working solution in a concentration range from 10 ppm to 40 ppm. Figure 8a illustrates that the use of DAHAPZ significantly reduced the corrosion rate at all concentrations. However, this reduction was stopped after 5 hours at concentrations of 10 and 20 ppm. The minimum corrosion rate at concentrations of 10 and 20 ppm was about 0.9 and 0.4 mm/year, respectively. As presented in Figure 8a, the optimal effective concentration of DAHAPZ was 30 ppm. At this concentration, the corrosion rate was 0.04 mm/year, which represents a 98% reduction in the corrosion rate. At higher concentrations (over 30 ppm), any further increase in the concentration of DAHAPZ would not lead to a decrease in the corrosion rate. In addition, Figure 8b presents the error bar for the corrosion rate data in the absence of DAHAPZ.
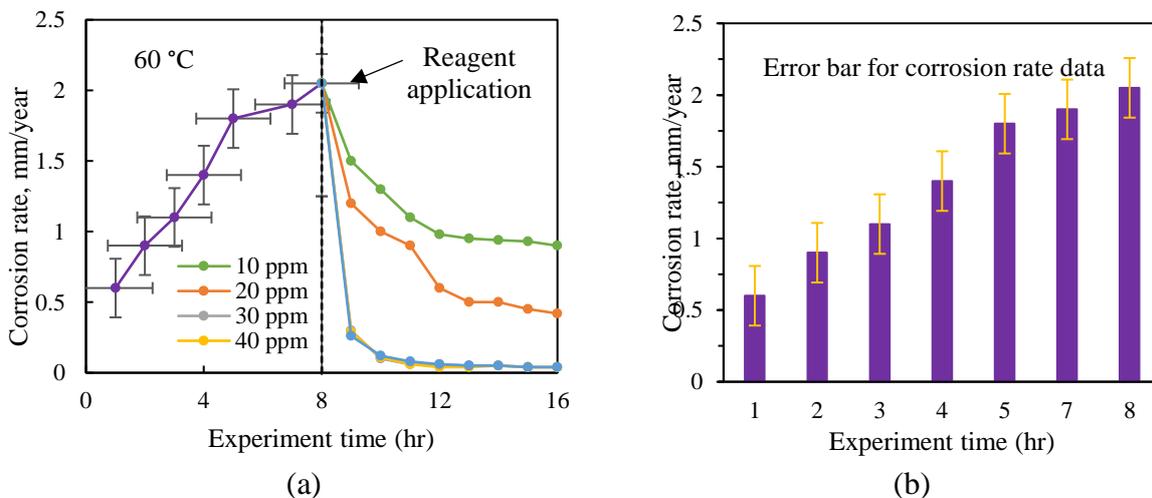
Fig. 8. The corrosion rate of the carbon steel samples in the presence and absence of DAHAPZ at different concentrations (a), and the error bar for the corrosion rate data (b)

Fig. 9 presents the results of the impedance spectrum tests using DAHAPZ at concentrations of 10, 20, 30, and 40 ppm. As shown in the figure, the corrosion inhibition efficiency was considerably increased by increasing the concentration of DAHAPZ. A larger arc radius can be achieved with an increase in the inhibitor concentration. Figure 9 shows that the optimal concentration of DAHAPZ for effective corrosion control was 30 ppm. The arc radius was approximately the same at concentrations of 30 and 40 ppm of DAHAPZ. Thus, the results showed that 30 ppm is an effective and optimal concentration of DAHAPZ for preventing corrosion and salt precipitation in the petroleum industry. DAHAPZ created the thinnest protective layers that prevent the destruction of the metal surfaces due to corrosion. It should

be noted that the inhibiting properties of DAHAPZ for preventing corrosion were manifested in a change in the surface state of the carbon steel samples.
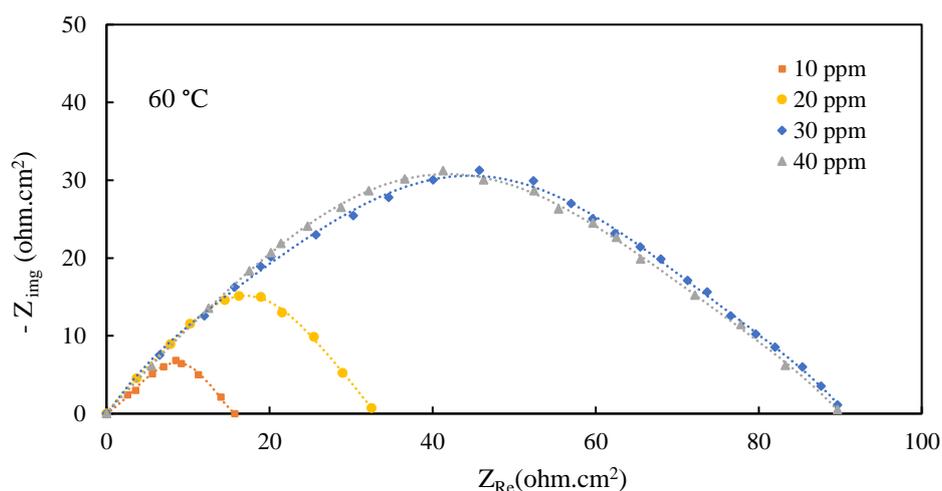
Fig. 9. The impedance spectrum in the presence of DAHAPZ at various concentrations

The Effect of Temperature on the Inhibition Performance of DAHAPZ

Temperature is one of the most important factors influencing the performance of the scale and corrosion inhibitors. Temperature changes can affect the solubility of inorganic salts in brines. Therefore, the inhibition efficiency of DAHAPZ in preventing calcium carbonate, barium sulfate, calcium sulfate and corrosion was evaluated at various temperatures. The results of the inhibition performance of DAHAPZ at temperatures of 40, 60, 80, 100 and 120 °C are shown in Table 4. The experiments were carried out at a constant concentration of 30 ppm of DAHAPZ. As presented in the table, the inhibition efficiency of DAHAPZ was not changed significantly by changing the temperature and remained above 90% at any investigated temperature. This behavior of DAHAPZ is associated with the effective inhibition mechanism to prevent corrosion and salt precipitation, as well as the appearance of a positive synergistic effect. Furthermore, the changes in the temperature did not affect the protective layers against corrosion on the surface of the carbon steel samples and the adsorption of the scale inhibitors on the salt crystals. Also, DAHAPZ inhibited the salt crystals, serving as a protective barrier, thereby reducing the corrosion rate at the studied temperatures.

Table 4. The effect of temperature on the inhibition performance of DAHAPZ at 30 ppm

Temperature (°C)	Inhibition performance (%)			
	SIE-CaCO$_3$	SIE-BaSO$_4$	SIE-CaSO$_4$	CIE
40	92.3	93.2	91.9	92.6
60	93.1	93.4	92.4	92.7
80	92.6	93.5	91.4	92.4
100	92.5	93.5	91.5	92.6
120	92.1	93.4	91.7	92.4

The Results of Turbidity Test and Salt Precipitation Before and After DAHAPZ Application

High turbidity of brines indicates the presence of small impurities and insoluble or colloidal particles of the formed salts. The turbidity value is increased due to an increase in the amount of salt precipitation. Fig. 10 depicts the results of the turbidity test with and without the use of DAHAPZ in the brines. The tests were conducted at a constant concentration of 30 ppm for 200 min. As shown in the figure, in the absence of DAHAPZ, the turbidity value was increased over time in all brines. It relates to the salt precipitation in the brines in the absence of DAHAPZ.

When the reagent was added to the brines, the turbidity value remained constant at a low level and was not changed during the experiments. Figure 10 shows the high inhibition efficiency of DAHAPZ for preventing salt precipitation ($CaCO_3$, $BaSO_4$, and $CaSO_4$) in all brines. This behavior of DAHAPZ is associated with the inhibition mechanism that could effectively prevent salt precipitation.
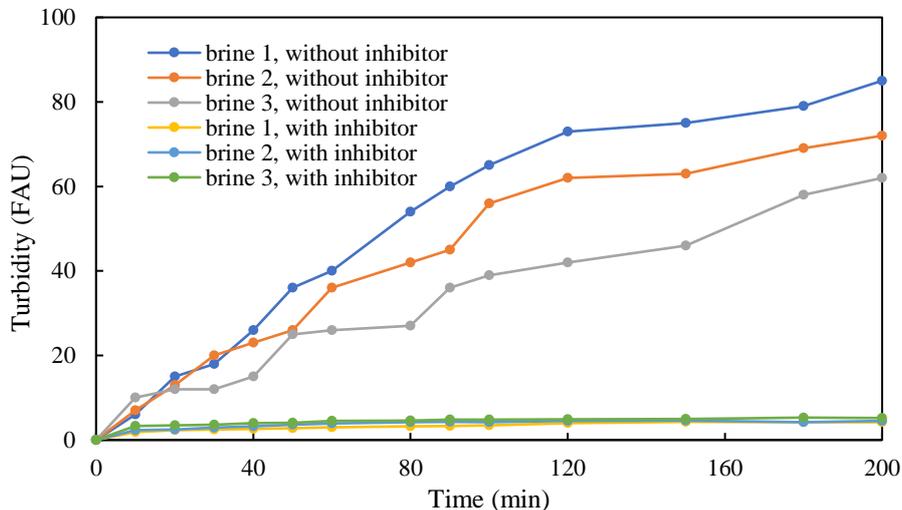
Fig. 10. The changes in the turbidity values in the brines with and without the use of DAHAPZ at a concentration and temperature of 30 ppm and 60 °C

Fig. 11 presents the results of the salt precipitation tests that were completed in order to evaluate the inhibition performance of DAHAPZ in preventing salt precipitation under static conditions. In the tests, the amount of precipitated salt in the working solutions (brines) was analyzed before and after the use of DAHAPZ. The tests were carried out at a constant temperature of 60 °C. DAHAPZ was used at a concentration of 30 ppm. The experiment duration for each test was 24 hours. As shown in the figure, calcium carbonate (in brine No.1), barium sulfate (in brine No.2), and calcium sulfate (in brine No.3) were formed and precipitated in the absence of DAHAPZ. Thus, a significant amount of salt precipitation (20.8–24.3 wt.%) was observed in all brines. After adding DAHAPZ to the working solutions, the concentrations of the precipitated salts were reduced significantly, indicating the high efficiency of DAHAPZ in preventing CaCO3, BaSO4, and CaSO4 salts. This high efficiency relates to the reduction in the crystal growth rate of calcium carbonate, barium sulfate, and calcium sulfate in the presence of DAHAPZ. The approach to explaining the deceleration of the crystal growth rate using DAHAPZ is associated with efficient adsorption on the crystals, and a decrease in the surface area of the crystals for growth. It should be noted that the mechanism of DAHAPZ for scale inhibition was not examined. In this work, the aim was to develop a scheme (experimentally routine and time-wise) to evaluate the efficiency of the suggested package. Considering what we have observed so far, which shows a very good efficiency, performing more advanced tests would be a topic of further/future analysis, in which we will aim to unravel the microscopic and molecular level mechanism of scale and corrosion inhibition using the present package. Based on the results obtained in the previous works, the main mechanism for DTPMP and HEDP is the prevention of crystal growth, and for ATMP is the decrease in nucleation [57, 58].
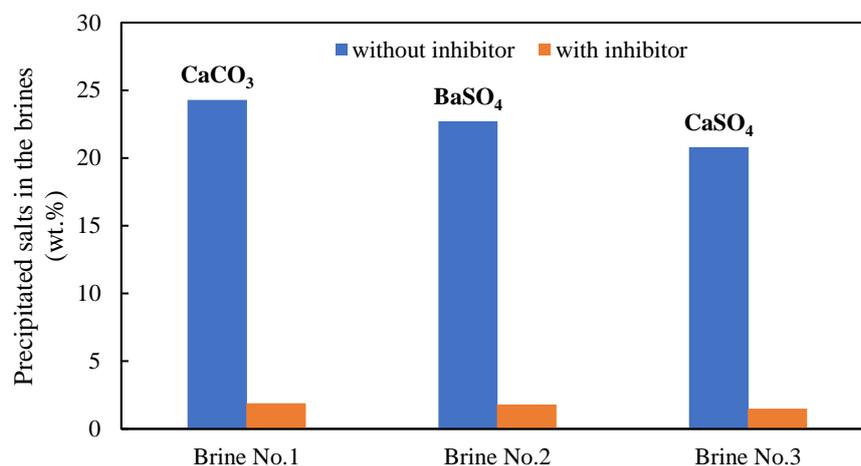
Fig. 11. The amount of precipitated salts with and without the use of DAHAPZ at 60 °C and 30 ppm in the static tests

The Changes in the Concentration of DAHAPZ onto the Carbonate and Sandstone Rock Samples

In the adsorption process, a sufficient amount of inhibitor should be adsorbed onto the rock surface to prevent corrosion and salt precipitation over a long period in the near-wellbore region and production equipment. For this purpose, the changes in the concentration of DAHAPZ on the rock surfaces were evaluated under dynamic conditions. Inhibitor adsorption on the rock surface was determined by measuring the phosphate ion concentration at the outlet of the coreholder by the titration method. This method could measure only the phosphonate scale inhibitor concentration, and could not provide any information about the concentration of corrosion inhibitors in the developed package. Figure 12 illustrates the results of the inhibitor concentration profile on the surface of the carbonate and sandstone rocks in the coreflood experiments. These experiments were conducted at 60 °C. The experiments consist of the following two steps: i) injection of the brine into the core samples with the use of DAHAPZ at a concentration of 30 ppm (for adsorption process); ii) injection of the brine into the core samples without the use of DAHAPZ after the first step (for desorption process).

As shown in Figure 12, during the adsorption process (first step), the adsorption of DAHAPZ was increased sharply with time. In this case, the maximum amount of inhibitor adsorption onto the carbonate and sandstone rocks was about 14 and 2.8 mg/Kg rock. The high degree of the adsorption onto the carbonate samples is associated with the interaction of this type of rock with the components of DAHAPZ. In addition, the desorption process (second step) was examined to determine the inhibition performance in the protection against corrosion and scaling under dynamic conditions. Crystal growth can be effectively inhibited when the desorption kinetics are slow for a long production time. As presented in Figure 12, the desorption process in the sandstone rocks was completed faster than in the carbonate rocks. In the carbonate samples at the end of the experiment, the amount of inhibitor onto the rock surfaces was about 1 mg/Kg rock. But in the sandstone samples, the minimum value was about 0.1 mg/Kg rock, which was much less than in the carbonate samples. Also, the minimum amount of inhibitor adsorption was observed faster in the sandstone samples than in the carbonate samples. The results show that DAHAPZ can be effectively used in carbonate reservoirs for preventing both corrosion and salt precipitation. Therefore, DAHAPZ can be recommended for use in carbonate reservoirs where corrosion and precipitation of calcium carbonate, calcium sulfate, and barium salts are observed due to the high concentration of ions in the formation of water.
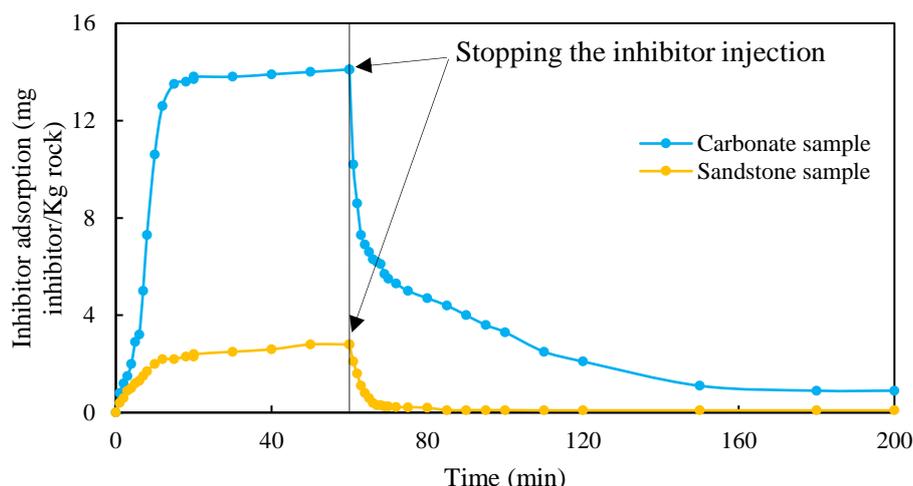
Fig. 12. The changes in the concentration of DAHAPZ in the carbonate and sandstone rock samples at 60 °C and 30 ppm

Conclusions

To effectively inhibit the corrosion and salt precipitation (calcium carbonate, barium sulfate, and calcium sulfate), a new mixture of reagents was developed containing the following components: DTPMP (16.6%), ATMP (16.7%), HEDP (16.7%), 2-aminoN-decyl-3-phenyl propionamide (25%), 2-propyl-3-ethyl-8-oxychinolin – $ZnCl_2$ (25%). The inhibition efficiency of DAHAPZ under static conditions was greater than 92% in preventing both salt and corrosion. The high efficiency of DAHAPZ relates to the appearance of a positive synergistic effect among its components, which provided the required inhibitory ability. DAHAPZ inhibited the salt crystals, which could serve as a protective barrier, thereby reducing the corrosion rate at the investigated temperatures. Based on the results obtained in the corrosion rate and EIS tests, the optimal concentration of DAHAPZ was 30 ppm. The corrosion rate of the carbon steel samples was decreased from 2 mm/year to 0.04 mm/year after the application of DAHAPZ.

As the temperature rises from 60 °C to 120 °C, the inhibition performance of DAHAPZ for preventing corrosion and calcium carbonate, barium sulfate, calcium sulfate precipitation remains above 92% at any studied temperature.

The turbidity values were significantly reduced after adding DAHAPZ to the brines at a constant concentration of 30 ppm. Moreover, with the use of DAHAPZ, the concentration of $CaCO_3$, $BaSO_4$, and $CaSO_4$ precipitation was reduced from 24.3, 22.7, 20.8 wt.% to 1.9, 1.8, 1.5 wt.%, respectively. The deceleration of the crystal growth rate when using DAHAPZ is associated with effective adsorption on the crystals, and a decrease in the crystal surface area for growth.

The amount of adsorption of DAHAPZ on the surface of the carbonate samples was higher than on the sandstone samples under dynamic conditions. Also, the desorption process in the carbonate samples has lasted longer than in the sandstone samples. Thus, DAHAPZ is recommended to be used in carbonate reservoirs, in which corrosion and salt precipitation occur.

Nomenclature

A	Surface area of the samples (m^2)
CIE	Corrosion inhibition performance (%)
K_{f2}	Final concentrations of the cations with reagents (ppm)

K_{f1}	Final concentrations of the cations without reagents (ppm)
K_i	Initial concentration of cations (ppm)
m_f	Mass of the carbon steel samples after test (gr)
m_i	Masse of the carbon steel samples before test (gr)
R_{corr}	Corrosion rate (mm/year)
SIE	Scale inhibition performance (%)
t	Test duration (hr)
ρ	Density of the samples (kg/m^3)

Abbreviations

ATMP	Amino trimethylene phosphonic acid
CI	Corrosion inhibitor
DAHAPZ	New developed mixture of reagents
DTPMP	Diethylenetriamine penta
EIS	Electrochemical impedance spectroscopy
HDTMP	Hexamethylenediaminotetra (methylene phosphonic acid)
HEDP	Hydroxyethylidenediphosphonic acid
MTBF	Mean time between failures
PBTC	2-phosphonobutane-1,2,4- tricarboxylic acid
SI	Scale inhibitor

References

[1]   Oddo JE, Tomson MB. Why scale forms in the oil field and methods to predict it. SPE Production & Facilities. 1994 Feb 1;9(1):47-54.

[2]   Olajire AA. A review of oilfield scale management technology for oil and gas production. Journal of Petroleum Science and Engineering. 2015 Nov 1;135:723-37.

[3]   Wylde JJ, Turner N, Austill M, Okocha C, Obeyesekere N. Development, testing and field application of a novel combination foamer-iron sulfide scale inhibitor-corrosion inhibitor in east Texas. In SPE International Symposium on Oilfield Chemistry. Montgomery, Texas, USA;2017 April 3.

[4]   Wang Q, Liang F, Al-Nasser W, Al-Dawood F, Al-Shafai T, Al-Badairy H, Shen S, Al-Ajwad H. Laboratory study on efficiency of three calcium carbonate scale inhibitors in the presence of EOR chemicals. Petroleum, 2018 Dec 1;4(4):375-84.

[5]   Macedo RGMDA, Marques NDN, Paulucci LCS, Cunha JVM, Villetti MA, Castro BB, Balaban RDC. Water-soluble carboxymethylchitosan as green scale inhibitor in oil wells. Carbohydrate Polymers. 2019 July 1;215:137-42.

[6]   Nikoo AH, Malayeri MR. On the affinity of carbonate and sandstone reservoir rocks to scale formation – Impact of rock roughness. Colloids and Surfaces A: Physicochemical and Engineering Aspects. 2021 Feb 5;610:Article 125699.

[7]   Amro MM. Effect of scale and corrosion inhibitors on well productivity in reservoirs containing asphaltenes. Journal of Petroleum Science and Engineering. 2005 April 30;46(4):243-52.

[8]   Khormali A, Petrakov DG. Laboratory investigation of a new scale inhibitor for preventing calcium carbonate precipitation in oil reservoirs and production equipment. Petroleum Science. 2016 May 1;13:320-7.

[9]   Li M, Dai C, Yang B, Qiao Y, Zhu Z. New and green multi-component scaling and corrosion inhibitor for the cooling water of central air conditioners. Journal of Materials Engineering and Performance. 2017 Feb 1;26:764-72.

[10]   Mpelwa M, Tang SF. State of the art of synthetic threshold scale inhibitors for mineral scaling in the petroleum industry: a review. Petroleum Science. 2019 Aug 2;16:830-49.

[11]   Obot IB, Onyeachu IB, Umoren SA, Quraishi MA, Sorour AA, Chen T, Aljeaban N, Wang Q. High temperature sweet corrosion and inhibition in the oil and gas industry: Progress, challenges

and future perspectives. Journal of Petroleum Science and Engineering. 2020 Feb 1;185:Article 106469.

[12] Liu X, Sheng X, Yao Q, Zhao L, Xu Z, Zhou Y. Synthesis of a new type of 2-phosphonobutane-1,2,4-tricarboxylic-acid-modified terpolymer scale inhibitor and its application in the oil field. Energy & Fuels, 2021 Mar 17;35(7):6136-43.

[13] Zhang P, Liu Y, Zhang N, Fai lp W, Kan AT, Tomson MB. A novel attach-and-release mineral scale control strategy: Laboratory investigation of retention and release of scale inhibitor on pipe surface. Journal of Industrial and Engineering Chemistry. Chem. 2019 Feb 25;70:462-71.

[14] Ruan G, Kan AT, Tomson MB, Zhang P. Facile one-pot synthesis of metal-phosphonate colloidal scale inhibitor: Synthesis and laboratory evaluation. Fuel. 2020 Dec 15;282:Article 118855.

[15] Kan AT, Dai Z, Tomson MB. The state of the art in scale inhibitor squeeze treatment. Petroleum Science. 2020 Dec 1;17:1579-601.

[16] Mady MF, Bayat P, Kelland MA. Environmentally friendly phosphonated polyetheramine scale inhibitors - excellent calcium compatibility for oilfield applications. Industrial & Engineering Chemistry Research. 2020 May 4;59(21):9808-18.

[17] Kumar S, Naiya TK, Kumar T. Developments in oilfield scale handling towards green technology-A review. Journal of Petroleum Science and Engineering. 2018 Oct 1;169:428-44.

[18] Li S, Qu Q, Li L, Xia K, Li Y, Zhu T. Bacillus cereus s-EPS as a dual bio-functional corrosion and scale inhibitor in artificial seawater. Water Research. 2019 Dec 1;166:Article 115094.

[19] Abdel-Gaber AM, Abd-El-Nabey BA, Khamis E, Abd-El-Khalek DE. A natural extract as scale and corrosion inhibitor for steel surface in brine solution. Desalination. 2011 Sep 1;278(1-3):337-42.

[20] Ahmed MEM, Saad MA, Hussein IA, Onawole AT, Mahmoud M. Pyrite scale removal using green formulations for oil and gas applications: Reaction kinetics. Energy & Fuels. 2019 April 2;33(5):4499-505.

[21] Zhang W, Li HJ, Chen L, Sun J, Ma X, Li Y, Liu C, Han X, Pang B, Wu YC. Performance and mechanism of a composite scaling–corrosion inhibitor used in seawater: 10-Methylacridinium iodide and sodium citrate. Desalination. 2020 July 15;486;Article 114482.

[22] Meriem-Benziane,M., Bou-Saïd B, Nasser Muthanna BG, Boudissa I. Numerical study of elbow corrosion in the presence of sodium chloride, calcium chloride, naphthenic acids, and sulfur in crude oil. Journal of Petroleum Science and Engineering. 2021 March 1;198:Article 108124.

[23] Farhadian A, Rahimi A, Safaei N, Shaabani A, Abdouss M, Alavi A. A theoretical and experimental study of castor oil-based inhibitor for corrosion inhibition of mild steel in acidic medium at elevated temperatures. Corrosion Science. 2020 Oct 1;175:Article 108871.

[24] Kittel J, Ropital F, Grosjean F, Sutter EMM, Tribollet B. Corrosion mechanisms in aqueous solutions containing dissolved H_2S. Part 1: Characterisation of H_2S reduction on a 316L rotating disc electrode. Corrosion Science. 2013 Jan 1;66:324-9.

[25] Popoola LT, Grema AS, Latinwo GK, Gutti B, Balogun AS. Corrosion problems during oil and gas production and its mitigation. International Journal of Industrial Chemistry. 2013 Sep 27;4(35):1-15.

[26] Al-Sabagh AM, El Basiony NM, Sadeek SA, Migahed MA. Scale and corrosion inhibition performance of the newly synthesized anionic surfactant in desalination plants: Experimental, and theoretical investigations. Desalination. 2018 July 1;437:45-58.

[27] Zhu T, Wang L, Sun W, Yang Z, Wang S, Zhou Y, He S, Wang Y, Liu G. Corrosion-induced performance degradation of phosphorus-containing scale inhibitors at carbon steel-water interface. Industrial & Engineering Chemistry Research. 2018 March 22;57(14):5183-9.

[28] Bilousova NA, Herasymenko YS, Red'ko RM, Vasyl'ev HS, Vorobiova VI. Inhibitor protection of steel against corrosion and scaling under the influence of ultrasound. Materials Science. 2020 Oct 9;55:831-9.

[29] Quraishi MA, Ansari FA. Inhibitive effect of some gemini surfactants as corrosion inhibitors for mild steel in acetic acid media. Arabian Journal for Science and Engineering. 2011 Jan 6;36:11-20.

[30]   Finsgar M, Jackson J. Application of corrosion inhibitors for steels in acidic media for the oil and gas industry: A review. Corrosion Science. 2014 Sep 1;86:17-41.

[31]   Gutierrez ME, Gaona SJ., Calvete FE, Botett JA, Ferrari JV. Effect of scaling and corrosion inhibitors on the static adsorption of an anionic surfactant on a carbonate rock. In SPE International Symposium on Oilfield Chemistry. Galveston, Texas, USA;2019 March 29.

[32]   Liu Y, Zhang Y, Yuan J. Influence of produced water with high salinity and corrosion inhibitors on the corrosion of water injection pipe in Tuha oil field. Engineering Failure Analysis. 2014 Oct 1;45:225-33.

[33]   Liu G, Xue M, Yang H. Polyether copolymer as an environmentally friendly scale and corrosion inhibitor in seawater. Desalination. 2017 Oct 1;419:133-40.

[34]   Shaw SS, Sorbie KS. Synergistic properties of phosphonate and polymeric scale-inhibitor blends for barium sulfate scale inhibition. SPE Production & Operations. 2015 Feb 1;30(1):16-25.

[35]   Nikoo AH, Mahmoodi L, Malayeri MR, Kalantariasl A. Gypsum-brine-dolomite interfacial interactions in the presence of scale inhibitor. Chemical Engineering Science. 2020 Aug 31;222:Article 115718.

[36]   Mpelwa M, Tang SF. State of the art of synthetic threshold scale inhibitors for mineral scaling in the petroleum industry: A review. Petroleum Science. 2019 Aug 2;16:830-49.

[37]   Farooqui N, Sorbie KS. Oilfield scale inhibitors for application in precipitation squeeze treatments: Solubility of the Ca_PPCA complex. In SPE International Oilfield Scale Conference and Exhibition. Aberdeen, Scotland;2014 May 14.

[38]   Javidi M, Chamanfar R, Bekhrad S. Investigation on the efficiency of corrosion inhibitor in CO_2 corrosion of carbon steel in the presence of iron carbonate scale. Journal of Natural Gas Science and Engineering. 2019 Jan 1;61:197-205.

[39]   Chauhan DS, Verma C, Quraishi MA. Molecular structural aspects of organic corrosion inhibitors: Experimental and computational insights. Journal of Molecular Structure. 2021 March 5;1227:Article 129374.

[40]   Yang W, Feng W, Liao Z, Yang Y, Miao G, Yu B, Pe, X. Protection of mild steel with molecular engineered epoxy nanocomposite coatings containing corrosion inhibitor functionalized nanoparticles. Surface and Coatings Technology. 2021 Jan 25;406:Article 126639.

[41]   Hou BS, Zhang QH, Li YY, Zhu GY, Lei Y, Wang X, Liu HF, Zhang GA. In-depth insight into the inhibition mechanism of pyrimidine derivatives on the corrosion of carbon steel in CO_2-containing environment based on experiments and theoretical calculations. Corrosion Science. 2021 April 1;181:Article 109236.

[42]   Awad MK, Mustafa MR, Elnga MMA. Computational simulation of the molecular structure of some triazoles as inhibitors for the corrosion of metal surface. Journal of Molecular Structure: THEOCHEM. 2010 Nov 15;959(1-3):66-74.

[43]   Dong S, Yuan X, Chen S, Zhang L, Huang T. A novel HPEI-based hyperbranched scale and corrosion inhibitor: construction, performance, and inhibition mechanism. Industrial & Engineering Chemistry Research. 2018 Oct 2;57(42):13952-61.

[44]   Vorobyova V, Skiba M. Peach pomace extract as efficient sustainable inhibitor for carbon steel against chloride-induced corrosion. Journal of Bio- and Tribo-Corrosion. 2020 Nov 16;7:Article 11.

[45]   Sabzi R, Arefinia R. Investigation of zinc as a scale and corrosion inhibitor of carbon steel in artificial seawater. Corrosion Science. 2019 June 1;153:292-300.

[46]   Xu Y, Guo X, Chen N, Zhang L, Zhao W. Synthesis and corrosion inhibitory effect of a novel β-amino alcohol compound. Colloids and Surfaces A: Physicochemical and Engineering Aspects. 2021 Feb 5;610:Article 125974.

[47]   Chen J, Chen F, Han J, Su M, Li Y. Evaluation of scale and corrosion inhibition of modified polyaspartic acid. *Chemical Engineering & Technology*. 2020 Feb 25;43(6):1048-58.

[48]   Spicka K, Johnston CJ, Jordan MM, Nguyen L, Linares-Samaniego S, Sutherland L. The impact of organic acid on scale inhibitor/corrosion inhibitor interaction, a case study from West Africa. In SPE International Symposium on Oilfield Chemistry. The Woodlands, Texas, USA;2011 April 11.

[49]   Fu L, Lv J, Zhou L, Li Z, Tang M, Li J. Study on corrosion and scale inhibition mechanism of polyaspartic acid grafted β-Cyclodextrin. Materials Letters. 2020 April 1;264:Article 127276.

[50] Yao J, Ge H, Zhang Y, Wang X, Xie S, Sheng K, Meng X, Zhao Y. Influence of pH on corrosion behavior of carbon steel in simulated cooling water containing scale and corrosion inhibitors. Materials and Corrosion. 2020 Feb 25;71(8):1266-75.

[51] Zhang W, Li HJ, Chen L, Sun J, Ma X, Li Y, Liu C, Han X, Pang B, Wu YC. Performance and mechanism of a composite scaling–corrosion inhibitor used in seawater: 10-Methylacridinium iodide and sodium citrate. Desalination. 2020 July 15;486:Article 114482.

[52] Coto B, Martos C, Peña JL, Rodríguez R, Pastor G. Effects in the solubility of $CaCO_3$: Experimental study and model description. Fluid Phase Equilibria. 2012 June 25;324:1–7.

[53] Khormali A, Sharifov AR, Torba DI. Investigation of barium sulfate precipitation and prevention using different scale inhibitors under reservoir conditions. International Journal of Engineering Transactions A: Basics. 2018 Oct 1;31(10):1796-802.

[54] Khormali A, Sharifov AR, Torba DI. Increasing efficiency of calcium sulfate scale prevention using a new mixture of phosphonate scale inhibitors during waterflooding. Journal of Petroleum Science and Engineering. 2018 May 1;164:245-58.

[55] Baugh TD, Lee J, Winters K, Waters J, Wilcher J. A fast and information-rich test method for scale inhibitor performance. In SPE Offshore Technology Conference Offshore Technology Conference. Houston, Texas, USA;2012 April 30.

[56] Jiang Z, Li Y, Zhang Q, Hou B, Xiong W, Liu H, Zhang G. Purine derivatives as high efficient eco-friendly inhibitors for the corrosion of mild steel in acidic medium: Experimental and theoretical calculations. Journal of Molecular Liquids. 2021 Feb 1;323:Article 114809.

[57] Wang XX, Zhang TY, Dao GH, Xu ZB, Wu YH, Hu HY. Assessment and mechanisms of microalgae growth inhibition by phosphonates: Effects of intrinsic toxicity and complexation. Water Research. 2020 Nov 1;186:Article 116333.

[58] Rabizadeh T. The nucleation, growth kinetics and mechanism of sulfate scale minerals in the presence and absence of additives as inhibitors. PhD Thesis. The University of Leeds,UK;2016 Nov 1.